

RESEARCH ARTICLE

Open Access



Predictive model for epileptogenic tubers from all tubers in patients with tuberous sclerosis complex based on ^{18}F -FDG PET: an 8-year single-centre study

Zhongke Wang^{1†}, Yang Li^{2†}, Zeng He^{2†}, Shujing Li^{2†}, Kaixuan Huang², Xianjun Shi², Xiaoqin Sun², Ruotong Ruan³, Chun Cui⁴, Ruodan Wang⁵, Li Wang⁵, Shengqing Lv², Chunqing Zhang^{2,6}, Zhonghong Liu¹, Hui Yang^{2,6*}, Xiaolin Yang^{2*} and Shiyong Liu^{2,6*}

Abstract

Background More than half of patients with tuberous sclerosis complex (TSC) suffer from drug-resistant epilepsy (DRE), and resection surgery is the most effective way to control intractable epilepsy. Precise preoperative localization of epileptogenic tubers among all cortical tubers determines the surgical outcomes and patient prognosis. Models for preoperatively predicting epileptogenic tubers using ^{18}F -FDG PET images are still lacking, however. We developed noninvasive predictive models for clinicians to predict the epileptogenic tubers and the outcome (seizure freedom or no seizure freedom) of cortical tubers based on ^{18}F -FDG PET images.

Methods Forty-three consecutive TSC patients with DRE were enrolled, and 235 cortical tubers were selected as the training set. Quantitative indices of cortical tubers on ^{18}F -FDG PET were extracted, and logistic regression analysis was performed to select those with the most important predictive capacity. Machine learning models, including logistic regression (LR), linear discriminant analysis (LDA), and artificial neural network (ANN) models, were established based on the selected predictive indices to identify epileptogenic tubers from multiple cortical tubers. A discriminating nomogram was constructed and found to be clinically practical according to decision curve analysis (DCA) and clinical impact curve (CIC). Furthermore, testing sets were created based on new PET images of 32 tubers from 7 patients, and follow-up outcome data from the cortical tubers were collected 1, 3, and 5 years after the operation to verify the reliability of the predictive model. The predictive performance was determined by using receiver operating characteristic (ROC) analysis.

Results PET quantitative indices including SUVmean, SUVmax, volume, total lesion glycolysis (TLG), third quartile, upper adjacent and standard added metabolism activity (SAM) were associated with the epileptogenic tubers. The

[†]Zhongke Wang, Yang Li, Zeng He and Shujing Li contributed equally to this work as co-first authors.

*Correspondence:

Hui Yang
huiyangtg2018@aliyun.com
Xiaolin Yang
yangxl2013@163.com
Shiyong Liu
liushi24252016@163.com

Full list of author information is available at the end of the article



SUVmean, SUVmax, volume and TLG values were different between epileptogenic and non-epileptogenic tubers and were associated with the clinical characteristics of epileptogenic tubers. The LR model achieved the better performance in predicting epileptogenic tubers (AUC = 0.7706; 95% CI 0.70–0.83) than the LDA (AUC = 0.7506; 95% CI 0.68–0.82) and ANN models (AUC = 0.7425; 95% CI 0.67–0.82) and also demonstrated good calibration (Hosmer–Lemeshow goodness-of-fit p value = 0.7). In addition, DCA and CIC confirmed the clinical utility of the nomogram constructed to predict epileptogenic tubers based on quantitative indices. Intriguingly, the LR model exhibited good performance in predicting epileptogenic tubers in the testing set (AUC = 0.8502; 95% CI 0.71–0.99) and the long-term outcomes of cortical tubers (1-year outcomes: AUC = 0.7805, 95% CI 0.71–0.85; 3-year outcomes: AUC = 0.8066, 95% CI 0.74–0.87; 5-year outcomes: AUC = 0.8172, 95% CI 0.75–0.87).

Conclusions The ^{18}F -FDG PET image-based LR model can be used to noninvasively identify epileptogenic tubers and predict the long-term outcomes of cortical tubers in TSC patients.

Keywords Tuberous sclerosis complex, Epileptogenic tubers, Epilepsy, ^{18}F -FDG PET, Machine learning

Background

Tuberous sclerosis complex (TSC) is a rare autosomal dominant genetic syndrome with an incidence of 1 in 6000–22000 live births. Approximately 85% of TSC patients have TSC1 or TSC2 gene mutations, which cause overactivation of the mTOR signalling pathway. TSC is a typical cause of neurodevelopmental delay, and over 54% of TSC patients suffer from drug-resistant epilepsy (DRE) [1–3]. Our previous nationwide multicentre retrospective study reported the China expert consensus on the surgical treatment of TSC-related intractable epilepsy and showed that surgery is the most effective way to control intractable epilepsy in patients with TSC [4, 5]. Multiple cortical tubers are typical manifestations in patients with TSC, and a previous study showed that electrographic seizures originated from the cortical tubers and perituberal cortex [6]. Therefore, precise preoperative identification of epileptogenic tubers from all cortical tubers is the key to determining the resection approach, surgical outcomes, and prognosis for TSC-related epilepsy [7–9]. Epileptogenic tubers can be identified by comprehensive preoperative assessments, including neurological physical examinations, genetic tests, computed tomography (CT), magnetic resonance imaging (MRI), ^{18}F -fluorodeoxyglucose positron emission tomography/computed tomography (^{18}F -FDG PET/CT), scalp video-EEG and intracranial EEG monitoring [10]. Epileptic discharges on intracranial EEG monitoring are reliable signals for localizing epileptogenic tubers, but this procedure is invasive. Given growing evidence of the potential for imaging biomarkers to predict epileptogenic foci, noninvasive neuroimaging monitoring has become of increasing interest in identifying epileptogenic tubers in TSC patients.

The safety and efficacy of different imaging modalities for locating epileptogenic foci varies widely. PET is considered an essential noninvasive method for preoperative evaluation in epilepsy patients, as it can safely reflect dynamic, seizure-related metabolism, especially when

MRI and EEG monitoring are discordant or inconclusive [11, 12]. And machine learning based on ^{18}F -FDG PET images can be used to accurately lateralize and classify MRI-negative temporal lobe epilepsy [13]. Although ^{18}F -FDG PET has become an indispensable part of preoperative evaluations for TSC patients with intractable epilepsy, the precise localization of epileptogenic tubers based on ^{18}F -FDG PET images has not been fully evaluated due to a lack of systematic studies.

Quantitative ^{18}F -FDG PET analysis has been used to explore the distribution of hypometabolism in patients with focal epilepsy in different brain regions, as the resulting quantitative indices are an informative tool for identifying potential epileptogenic zones [14, 15]. Positive correlations have been identified between the maximum standard uptake value (SUV) and the frequency of lateralized periodic discharges in patients with intractable epilepsy [16], and quantitative ^{18}F -FDG PET asymmetry features predict long-term seizure recurrence in refractory epilepsy. Our previous research reported the SUVs could predict the localization of epileptogenic foci in patients with focal cortical dysplasia type IIb and TSC [17]. According to these results, we hypothesize the quantitative indices of ^{18}F -FDG PET would provide the potential value in identifying epileptogenic tubers in patients with TSC.

In this study, we constructed a predictive model based on ^{18}F -FDG PET images to accurately identify epileptogenic tubers from multiple cortical tubers before surgery, predict the long-term outcomes of epileptogenic tubers, and provide guidance to clinicians on precise surgical intervention in TSC.

Methods

Study design and cohorts

This study was approved by our institutional review board, and all subjects signed informed consent forms. We selected consecutive TSC patients who presented to

the comprehensive epilepsy center from June 2013 to July 2021. The inclusion criteria were (i) patients diagnosed with TSC according to the diagnostic criteria in 2021 [3]; (ii) intractable epilepsy and seizures occurring at least twice per month on average during the 6 months prior to surgery; (iii) comprehensive preoperative evaluations and epilepsy surgery at our comprehensive epilepsy centre; (iv) ^{18}F -FDG PET examination completed more than 48 h since the last seizure; and (v) at least 1 year of follow-up. The exclusion criteria were (i) patients with other specific neurological abnormalities, mainly including encephalitis, hydrocephalus, intracerebral haemorrhage or cerebrovascular disease; (ii) contraindications for imaging examinations; and (iii) who dropped out of the study or loss to follow-up. The study flowchart is presented in Fig. 1.

Clinical characteristics (including data on sex, age at onset, frequency of seizures, number of antiseizure medications [ASMs], and number of tubers) were collected. Comprehensive preoperative examinations, including neurological physical examinations, genetic tests, MRI, ^{18}F -FDG PET/CT, scalp video-EEG and stereoelectroencephalography (SEEG), were performed by neurosurgeons, neurologists and neuroradiologists to determine

whether and how to perform epilepsy surgery on the TSC patients. We first chose a noninvasive method to identify the epileptogenic tubers based on our and other previous studies [4, 18, 19]. An epileptogenic tuber was defined as (i) a cortical tuber with focal ictal and interictal epileptiform discharges in the same brain region on scalp EEG with consistent seizure symptoms; (ii) an outstanding cortical tuber with focal ictal or interictal epileptiform discharges in the same brain region on scalp EEG with consistent seizure symptoms; or (iii) an outstanding cortical tuber with focal ictal and interictal epileptiform discharges in the same brain region on scalp EEG. Outstanding cortical tubers described were defined as having a size > 3–4 cm and containing a nidus of calcification according to imaging results. For those patients with multiple epileptogenic cortical tubers or discrepancies among clinical symptoms, imaging results and electrophysiology findings, intracranial electrodes were invasively implanted to record electrical activity and identify epileptogenic tubers. In addition, resected “non-epileptogenic tubers” in this study are adjacent to epileptogenic tubers, exposed to the same surgical field with the epileptogenic tubers and located in the non-functional areas, and these tubers are large, prominent or calcified tubers

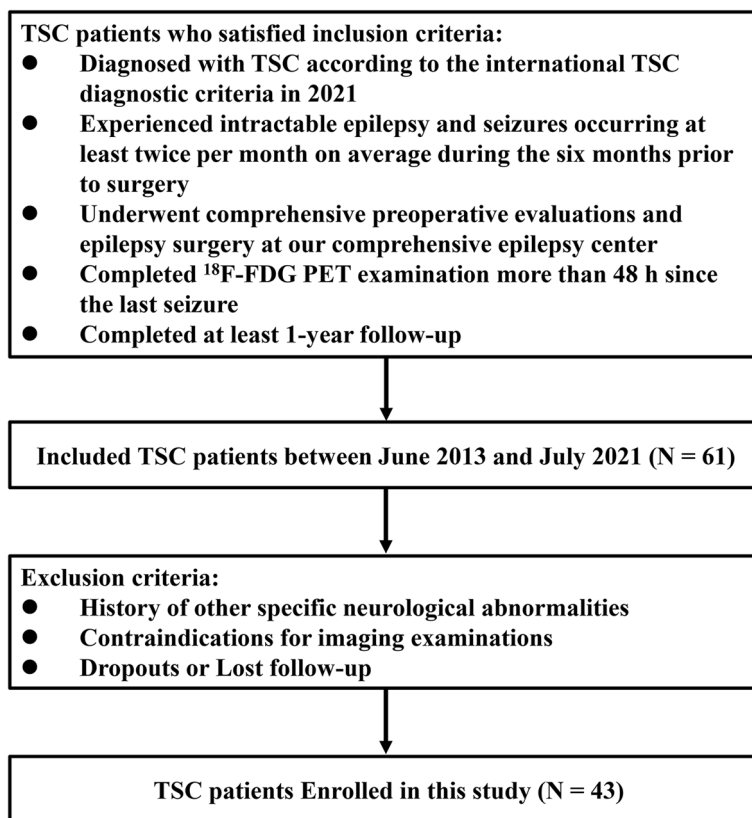


Fig. 1 Flow diagram. Flowchart shows the patient inclusion and exclusion criteria

but without epileptic discharges. These tubers have the potential to become epileptogenic tubers, strongly suggest pharmacoresistant epilepsy in TSC, influence post-operative seizure freedom and should be considered good indicators for epilepsy surgery [4, 20]. Patients finished their last follow-up in July 2022. The clinical characteristics of the patients are shown in Table 1.

Imaging data collection and processing

The criteria are summarized as follows: at least 4 h of fasting before FDG PET/CT, blood glucose level at the time of FDG injection < 11.1 mmol/L, and PET acquisition was done 1 h after the injection of 3 MBq/kg of FDG. In addition, MRI scans were performed with a 3.0-T system with a vendor-produced 32-channel head coil. Patients were in an awake, resting state, and no patients had seizures during the imaging scans. Image registration was utilized to spatially align the ¹⁸F-FDG PET and T2Flair MRI images using CT images as a reference, and the registered image showed the spatial correspondence between PET and MRI images (Additional file 1: Fig. S1, Step 1–2). Then, regions of interests (ROIs) were delineated on the T2Flair MRI images and the delineated ROIs also applied to the PET images (Additional file 1: Fig. S1, Step 3). The quantitative indices of the delineated ROIs were further extracted based on the PET images (Additional file 1: Fig. S1, Step 4). In each delineated ROI, 19 quantitative indices that reflect the clinical significance of the PET image were identified [17, 21–24]. A detailed explanation of these indices is shown in Additional file 1: Tab. S1. Researchers blinded to the clinical and imaging features delineated the ROIs and analysed the imaging data independently. All processing procedures were performed under the guidance of experienced PET/CT specialists.

Model development and evaluation

Logistic regression (LR), linear discriminant analysis (LDA) and artificial neural network (ANN) models were constructed using R 4.2.1 software (R Foundation for Statistical Computing, Vienna, Austria). ROC analysis was used to confirm the identification performance of all models. The relationship between the PET quantitative indices and the probability of identifying an epileptogenic tuber was visualized at the bottom of the nomogram. Calibration curves were used to assess the agreement between the predicted probability and the actual proportion, and the Hosmer–Lemeshow test was used to estimate the calibration of the nomogram model. In addition, decision curve analysis (DCA) and clinical impact curve (CIC) were performed to evaluate the utility of the nomogram.

Table 1 Clinical characteristics of patients with TSC (n = 43)

Characteristics	Values
Female/male	20(46.5)/23(53.5)
Type of variation	
TSC1	8(18.6)
TSC2	29(67.4)
No variation	6(14)
Age at onset (month)	20.16(1–156)
Frequency of seizure	
Per day	26(60.5)
Per week	10(23.2)
At least twice per month	7(16.3)
Number of AEDs	2.19(1–4)
Number of tubers	
1–3	8(18.6)
4–6	26(60.5)
> 6	9(20.9)
Ictal scalp EEG	
Focal	10(23.2)
Lateralized	12(27.9)
Multifocal	14(32.6)
Generalized	7(16.3)
Intracranial EEG	
Subdural electrode EEG	16(37.2)
Stereo-EEG	13(30.2)
No intracranial EEG	14(32.6)
Surgery approach	
(Multiple) tuberectomy	17(39.5)
(Multiple)lobectomy	11(25.6)
Lobectomy + tuberectomy	15(34.9)
Post-surgical seizure outcomes	
1 year follow ^a	SF 32(74.4) No-SF 11(25.6)
3 years follow ^b	SF 26(68.4) No-SF 12(31.6)
> 5 years follow ^c	SF 21(65.6) No-SF 11(34.4)

Abbreviations: TSC tuberous sclerosis complex, AED antiepileptic drug, SF seizure freedom

Values are n (%) or mean (range)

^a Available patient data n = 43

^b Available patient data n = 29

^c Available patient data n = 13

Western blot

The proteins of the resected brain tissues from TSC patients were extracted, and their concentration was measured using a BCA protein assay. The extracted protein was mixed with 5× loading buffer, electrophoresed in 10% sodium dodecyl sulfate polyacrylamide gel and transferred onto polyvinylidene difluoride membranes.

The membranes were then blocked in 5% skim milk for 2 h at room temperature. Then, the membranes were incubated with the primary antibodies overnight at 4 °C, including anti-mTOR (1:1000, Abcam) and anti-GAPDH (1:1000, Abcam). After washing, the membranes were incubated with anti-rabbit or anti-mouse secondary antibodies for 1 h at room temperature. Specific protein bands were visualized in the membranes using the chemiluminescence method, and the optical density of the protein bands was analysed in Image-Pro Plus software.

Statistics

Continuous variables were compared by the unpaired two-tailed *T* tests. The relationship between quantitative indices and epileptogenesis was evaluated using logistic regression analysis. Bivariate correlation analyses were carried out using Spearman's rank correlation test. Receiver operating characteristic curve (ROC) analysis was performed to evaluate the performance of the models. The area under the curve (AUC) was calculated to illustrate the diagnostic power of the models. A nomogram was built to help guide clinicians, and DCA was performed to evaluate the utility of the nomogram. R 4.2.1 software was used for data analysis. Significance was set at $P < 0.05$.

Results

Patient clinical characteristics

Data from 61 TSC patients who underwent epilepsy surgery in our centre were collected. Eighteen patients were excluded based on the exclusion criteria. Forty-three patients (20 female, 23 male) were ultimately enrolled in this study (Fig. 1).

The clinical characteristics of the TSC patients were collected (Table 1). According to gene testing, 8 patients had a TSC1 variant, 29 had a TSC2 variant and 6 patients had no gene variants. The average age at onset was 20.16 months (range 1–156 months). Seizures occurred every day in 26 patients, per week in 10 patients and at

least twice per month in 7 patients. The average number of ASMs was 2.19 (range 1–4). Eight patients had 1–3, twenty-six patients had 4–6 and nine patients had more than 6 cortical tubers. According to the ictal scalp EEG findings, 10, 12, 14 and 7 patients had focal, lateralized, multifocal and generalized epileptic discharges, respectively. Furthermore, 16 patients underwent subdural EEG monitoring, and 13 patients underwent SEEG monitoring. Tubectomy or multiple tubectomy was performed on 17 patients, lobectomy or multiple lobectomy was performed on 11 patients, and lobectomy plus tubectomy was performed on 15 patients. One-year follow-up was performed for all patients, and 32 patients were seizure-free. Three-year follow-up was performed for 38 patients, and 26 patients were seizure-free. An over-5-year follow-up was performed for 32 patients, and 21 patients were seizure-free.

Correlation between quantitative indices and epileptogenic tubers

Overall, 235 tubers (71 epileptogenic and 164 non-epileptogenic) from 43 patients were identified, and their PET quantitative indices were extracted and analysed. The results showed that the SUVmean, SUVmax, volume, total lesion glycolysis (TLG), third quartile, upper adjacent and standardized added metabolic activity (SAM) were associated with epileptogenic tubers (Table 2), and the SUVmean, SUVmax, volume, TLG and root-mean-square deviations (RMSD) values were different between epileptogenic tubers and non-epileptogenic tubers (Additional file 1: Tab. S2). Based on these results, we further selected the SUVmean, SUVmax, volume and TLG indices to investigate the association of PET quantitative indices and epileptic characteristics in TSC patients with a single epileptogenic tuber and found that SUVmean, SUVmax and TLG were negatively associated with seizure frequency and duration (Additional file 1: Fig. S2). Abnormal activation of the mTOR pathway is the pathogenic

Table 2 Relationship between quantitative indices and epileptogenic tubers in TSC patients

Quantitative indices	β	SE	Wald	<i>P</i> value	Exp(β)	95.0% CI	
SUVmean	-1.101	0.471	5.474	0.019*	0.332	0.132	0.836
SUVmax	-1.472	0.528	7.768	0.005**	0.229	0.082	0.646
Volume	0.911	0.330	7.608	0.006**	2.487	1.302	4.750
TLG	-0.454	0.124	13.300	0.000**	0.635	0.498	0.811
Third quartile	1.248	0.401	9.703	0.002**	3.484	1.589	7.643
Upper adjacent	1.188	0.529	5.037	0.025*	3.281	1.162	9.259
SAM	-0.448	0.194	5.314	0.021*	0.639	0.437	0.935

Abbreviations: SUV standard uptake value, TLG total lesion glycolysis, SAM standardized added metabolic activity

* $P < 0.05$, ** $P < 0.01$

mechanism of epilepsy in TSC [25]. Intriguingly, SUVmean and SUVmax were negatively associated with activated mTOR expression in resected epileptogenic tubers (Additional file 1: Fig. S3). The above results indicated that the PET quantitative indices have potential predictive value for epileptogenic tubers.

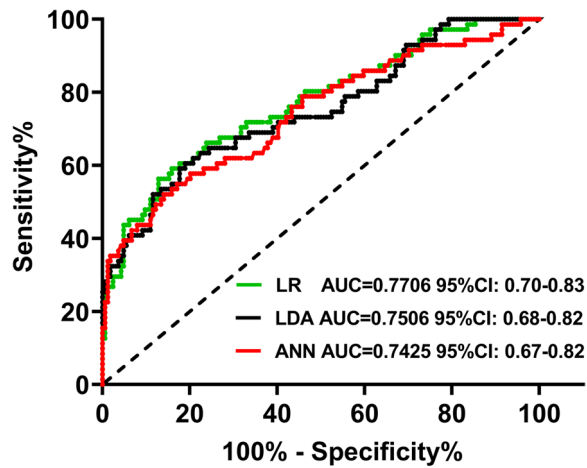


Fig. 2 Receiver operating characteristic (ROC) curves of LR, LDA and ANN models. ROC curves show the performance of LR models (AUC = 0.7706; 95% CI 0.70–0.83) is better than LDA (AUC = 0.7506; 95% CI 0.68–0.82) and ANN (AUC = 0.7425; 95% CI 0.67–0.82) models in identifying the epileptogenic tubers of TSC patients

Performance of identification models

The PET quantitative indices from 235 tubers were used as the training set. The AUCs of the training set in the LR, LDA and ANN predictive models were 0.7706 (95% CI, 0.70–0.83), 0.7506 (95% CI, 0.68–0.82) and 0.7425 (95% CI, 0.67–0.82), respectively (Fig. 2), indicating that the LR model performed better in predicting epileptogenic tubers than the LDA and ANN models (Fig. 2). The LR model was internally evaluated based on ten-fold cross-validation on discrimination and calibration, and the results showed that it was well calibrated (Hosmer–Lemeshow goodness-of-fit *p* value = 0.7). In addition, the multicollinearity of the PET quantitative indices was evaluated by the variance inflation factor (VIF), and the VIFs were less than 5, indicating that there was no multicollinearity in these models. Therefore, we selected the LR model to evaluate the values of the quantitative indices in predicting epileptogenic tubers.

Furthermore, a nomogram was constructed incorporating epileptogenic tuber-associated PET quantitative indices to guide clinicians in identifying epileptogenic tubers in TSC patients (Fig. 3A). Each patient was given points for each quantitative indices, and the higher the total points, the more likely the tuber was to be epileptogenic. In addition, calibration curves demonstrated that the nomogram had a similar performance to the ideal model and confirmed the good

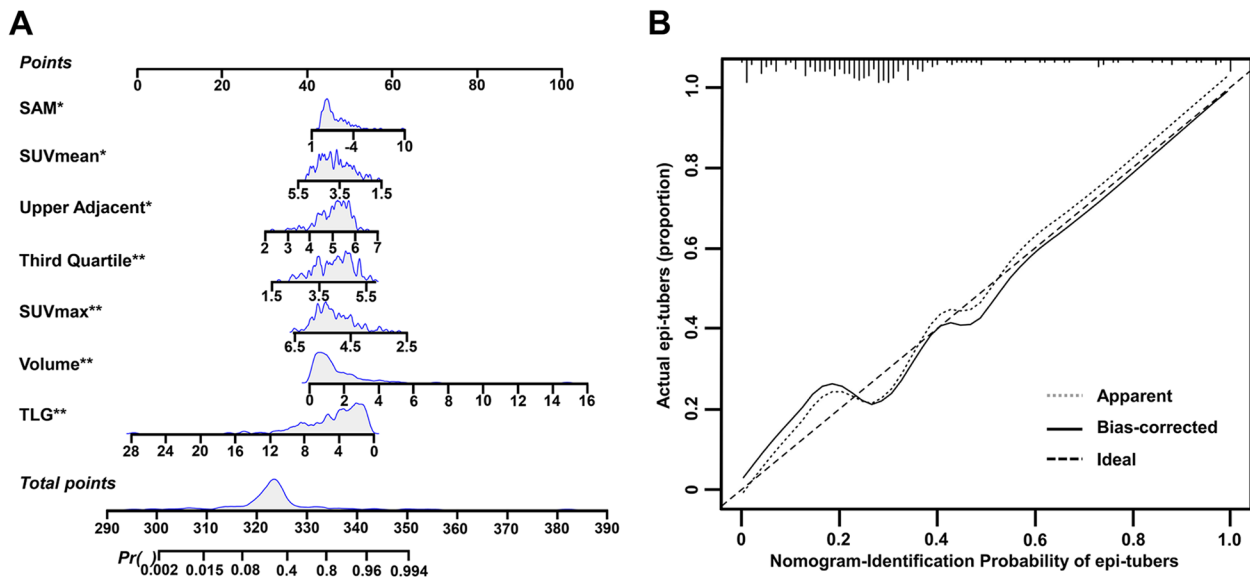


Fig. 3 Discriminating nomogram. **A** Nomogram makes accessible for clinicians to identify the epileptogenic tubers according to quantitative indices of ¹⁸F-FDG PET images. Gray density plots describe the distribution of epileptogenic tubers in quantitative indices and total points. **P* < 0.05, ***P* < 0.01. **B** Calibration curve for the nomogram to identify epileptogenic tubers. X-axis represents the nomogram-identification probability of epileptogenic tubers, and Y-axis represents the actual proportion of epileptogenic tubers. The diagonal dotted line indicates the best prediction by an ideal model. The apparent line represents the uncorrected performance of the nomogram, and the solid line shows the bias-corrected performance. 1000 bootstrap repetitions; mean absolute error = 0.046; *n* = 235

predictive capacity of the nomogram (Fig. 3B). DCA (Fig. 4A) and CIC (Fig. 4B) were established to confirm the clinical applicability of the nomogram. DCA showed that the prediction of epileptogenic tubers with the nomogram provide greater net benefits when the high-risk threshold probability was > 30%. CIC was used to predict the stratification of the probability of epileptogenic tubers for a sample size of 1000 and suggested that the number of identified epileptogenic tubers was close to the actual number of epileptogenic tubers when the threshold probability was higher than 0.4, and the cost-to-benefit ratio was 0.75.

Evaluation of the prediction model

New PET data of 32 tubers from 7 patients were used as the testing set to evaluate the predictability of the LR model. The AUC of the LR model was 0.8502 (95% CI, 0.71–0.99), and the accuracy was 78.13% (Table 3). Furthermore, we evaluated the prognostic value of the LR model in the long-term outcomes of cortical tubers based on the 1-, 3- and 5-year follow-up data. In the 1-year follow-up of 74 epileptogenic tubers, the AUC value was 0.7805 (95% CI, 0.71–0.85), and the accuracy was 79.15%. In the 3-year follow-up of 77 epileptogenic tubers, the AUC value was 0.8066 (95% CI, 0.74–0.87), and the accuracy was 80.43%. In the 5-year follow-up of 80 epileptogenic tubers, the AUC value reached 0.8172 (95% CI, 0.75–0.87), and the accuracy was 79.15% (Table 3). These findings showed the capability of the LR model to predict the long-term outcomes of cortical tubers.

Table 3 Identification of LR model to epileptogenic tubers in TSC patients

Characteristics	AUC	AUC 95%CI	Accuracy
Testing sets	0.8502	0.71–0.99	0.7813
1 year follow	0.7805	0.71–0.85	0.7915
3 years follow	0.8066	0.74–0.87	0.8043
5 years follow	0.8172	0.75–0.87	0.7915

Abbreviations: LR logistic regression, TSC tuberous sclerosis complex, AUC area under curve

Discussion

A quantitative predictive model for preoperatively identifying epileptogenic tubers in TSC patients based on ¹⁸F-FDG PET images is lacking. In this study, LR, LDA and ANN models were established based on the quantitative indices derived from ¹⁸F-FDG PET images and effectively identified epileptogenic tubers from all cortical tubers. ROC analysis showed that the LR model performed better in predicting epileptogenic tubers than the LDA and ANN models. A practical nomogram was constructed and showed good clinical applicability in identifying epileptogenic tubers according to DCA and CIC. Intriguingly, the LR model could also predict the long-term outcomes of cortical tubers. This study provided a noninvasive method for identifying epileptogenic tubers and predicting long-term outcomes of cortical tubers in patients with TSC.

Over the past three decades, ¹⁸F-FDG PET has been used to map patterns of brain glucose metabolism to evaluate brain function or demonstrate metabolism abnormalities in various brain disorders [26]. It is a

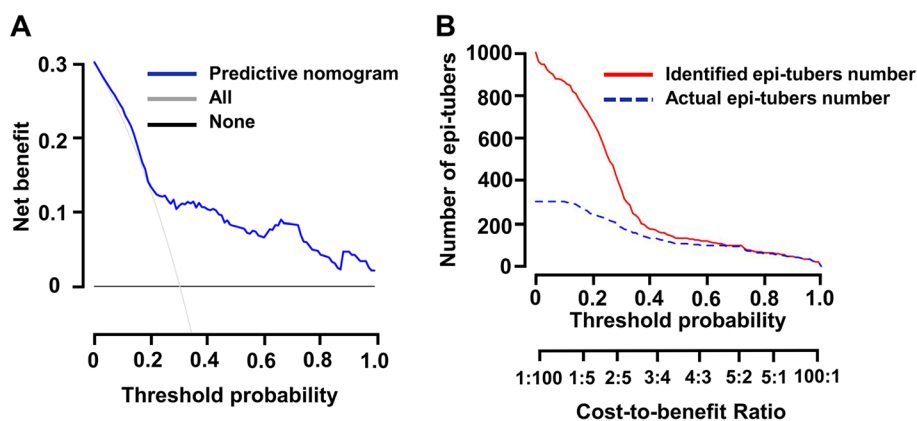


Fig. 4 Decision curve and clinical impact curve show identification probability of epileptogenic tubers using nomogram. **A** Decision curve for the probability of identifying epileptogenic tubers using nomogram. The net benefits were measured at different threshold probabilities. The blue line represents the identification nomogram. The gray line represents the assumption that all tubers are identified as epileptogenic tubers. The black line represents the assumption that no tubers are identified as epileptogenic tubers. **B** Clinical impact curve to identify the epileptogenic tubers for a population size of 1000. The red curve shows the identified number of epileptogenic tubers at different threshold probabilities, and the blue curve represents actual number of epileptogenic tubers

promising modality with high sensitivity, specificity and accuracy in detecting foci in patients with neurological diseases and is thought to have higher sensitivity than MRI [12]. Moreover, ^{18}F -FDG PET has been widely used in the presurgical assessment of patients with DRE by identifying the hypometabolic seizure onset zones, especially when MRI and scalp EEG are unable to do so or are discordant [11]. Previous studies have shown that interhemispheric metabolic asymmetry on interictal PET could indicate the location of the epileptogenic zone, and the oxygen-glucose index based on PET images showed unique value in identifying foci during the interictal period in patients with DRE [27, 28]. PET serves an important role in understanding the neuro-behavioural characteristics of TSC patients, including autism, attention deficit hyperactivity disorder and cognitive impairment, and it has become an indispensable, noninvasive clinical approach for preoperative evaluation in TSC patients with intractable epilepsy [29–32]. Notably, lower values of the PET quantitative indices SUV and TLG have been identified in lesions of FCDII patients than in contralateral and control regions, and ipsilateral relative SUVs were associated with increased lateralized periodic discharge frequency [16, 33]. Furthermore, our previous study confirmed that the SUVmax and SUVmean were significantly decreased in epileptogenic tubers [17]. In the current study, epileptogenic tubers had lower values for the quantitative indices SUVmax, SUVmean and TLG and a greater volume than non-epileptogenic tubers. Intriguingly, these quantitative indices were negatively correlated with seizure frequency, seizure duration and typical hyperactivation of the mTOR signalling pathway in TSC patients. Based on these results, we hypothesized that these PET quantitative indices had potential value in identifying epileptogenic tubers.

Further, LR, LDA and ANN predictive models were constructed based on the PET quantitative indices, and ROC analysis showed that the LR model had greater predictive value in identifying epileptogenic tubers than the LDA and ANN models. LR, a sensitive and stable binary prediction machine learning method, is widely used in feature-based classification, and it has been applied to single-neuron recordings from depth-electrode microwires to predict seizure onset zones [34, 35]. In addition, a predictive nomogram was constructed to make accurate localization assessments to quantitatively predict epileptogenic tubers in a personalized way. DCA is an appropriate method to evaluate alternative diagnosis and prognostic strategies by analyzing the clinical net benefit with a probability threshold and has previously been used for the withdrawal of antiseizure medications [36]. A previous study reported that DCA confirmed the usefulness and benefits of a clinical model for predicting seizure

freedom in MRI-negative epilepsy patients treated with antiseizure medications [37]. The DCA results further provided evidence of the usefulness and benefits of our predictive model.

Previous studies have shown that α -[(11)C]-methyl-L-tryptophan (AMT)-PET could pinpoint hypermetabolic epileptogenic tubers in approximately two-thirds of patients with tuberous sclerosis and intractable epilepsy, provide independent complementary information on the localization of epileptogenic regions in TSC and enhance the confidence of successful epilepsy surgery [38–40]. There are some limitations to the clinical promotion and application of AMT PET, including the very short half-life of its tracer and its low sensitivity in localizing epileptogenic tubers [41]. In contrast, ^{18}F -FDG PET is commonly used in clinical practice, but few studies have used it to identify epileptogenic tubers. We constructed the LR predictive model based on the quantitative indices of ^{18}F -FDG PET, achieving an AUC of 0.7706. New PET images from cortical tubers were used as a testing set to evaluate the predictive capability of the LR model; the AUC was 0.8502, and the accuracy was 78.13%. These results indicated that the ability of ^{18}F -FDG PET to identify epileptogenic tubers is comparable to that of AMT PET.

Some non-epileptogenic cortical tubers can potentially develop into epileptogenic tubers, but few studies have focused on the true outcomes of cortical tubers [4]. Thus, we explored the predictability of the LR model regarding the outcomes of cortical tubers using the follow-up data. Interestingly, the AUC and accuracy of the LR model improved with greater follow-up times, suggesting that the LR model could predict the outcomes of epileptogenic tubers and guide clinical intervention in TSC patients.

Conclusions

In conclusion, we developed a predictive LR model to identify epileptogenic tubers in TSC patients based on ^{18}F -FDG PET quantitative indices. Remarkably, the LR model also exhibited a promising ability to predict the longer-term outcomes of cortical tubers. The noninvasive predictive model can provide guidance for neurosurgical intervention in TSC, but further studies are required to confirm our findings in clinical practice.

Abbreviations

ANN	Artificial neural network
ASM	Antiseizure medication
AUC	Area under curve
CIC	Clinical impact curve
CT	Computed tomography
DCA	Decision curve analysis
DRE	Drug-resistant epilepsy

LDA	Linear discriminant analysis
LR	Logistic regression
MRI	Magnetic resonance imaging
PET	Positron emission tomography
RMSD	Root-mean-squared deviations
ROC	Receiver operating characteristic curve
ROI	Regions of interests
SAM	Standardized added metabolic
SEEG	Stereo-electroencephalogram
SUV	Standard uptake value
TLG	Total lesion glycolysis
TLG	Total lesion glycolysis
TSC	Tuberous sclerosis complex

Supplementary Information

The online version contains supplementary material available at <https://doi.org/10.1186/s12916-023-03121-0>.

Additional file 1: Table S1. The detailed explanation of Quantitative Indices. **Table S2.** ¹⁸F-FDG PET Quantitative Indices of Epileptogenic and Non-Epileptogenic tubers in TSC patients. **Figure S1.** Illustration shows the image processing pipeline and quantitative indices analysis based on ¹⁸F-FDG PET images. **Figure S2.** Relationship between the PET quantitative indices (SUVmean, SUVmax, Volume, TLG) and epileptic characteristics in TSC patients with single epileptogenic tuber. **Figure S3.** Relationship between the PET quantitative indices and mTOR expression in epileptogenic tubers.

Additional file 2: Figure S1. The original blot images of mTOR and GAPDH in Additional file 1 Fig. S3F.

Acknowledgements

The authors sincerely thank the patients and their families who participated in this study.

Authors' contributions

SYL, XLY, HY and ZKW were responsible for the study design and data interpretation. ZKW, YL, ZH, KXH and SJL participated in collection of study materials or patients. XJS, XQS, CC, RDW and LW participated in collection and assembly of data. ZKW, YL, ZH, XJS, XQS and RTR did the data analysis. SQL, COZ, ZHL, SYL and HY performed epilepsy surgery. ZKW, YL and ZH drafted the manuscript. SYL, XLY and HY proofread the manuscript for important intellectual content. All authors read and approved the final manuscript.

Funding

This work was supported by the National Natural Science Foundation of China (NO.82171448 and NO.82201613) and Natural Science Foundation of Chongqing (NO. CSTB2022NSCQ-MSX1550).

Availability of data and materials

The datasets used and/or analysed during the current study are available from the corresponding author on reasonable request.

Declarations

Ethics approval and consent to participate

All procedures in this study were performed according to the guidelines of the Declaration of Helsinki of the World Medical Association and the Ethics Committee guidelines of Xinqiao Hospital (approval number: RN395-01).

Consent for publication

Written informed consents were obtained from patients or their parents.

Competing interests

The authors declare that they have no competing interests.

Author details

¹Department of Neurosurgery, Armed Police Hospital of Chongqing, Chongqing, China. ²Department of Neurosurgery, Comprehensive Epilepsy Center, Xinqiao Hospital, Army Medical University, Chongqing, China. ³Department of Virology, State Key Laboratory of Pathogen and Biosecurity, Beijing Institute of Microbiology and Epidemiology, Beijing, China. ⁴Department of Radiology, Xinqiao Hospital, Army Medical University, Chongqing, China. ⁵Department of Neurology, Xinqiao Hospital, Army Medical University, Chongqing, China. ⁶Chongqing Institute for Brain and Intelligence, Guangyang Bay Laboratory, Chongqing, China.

Received: 13 May 2023 Accepted: 19 October 2023

Published online: 18 December 2023

References

- Curatolo P, Bombardieri R, Jozwiak S. Tuberous sclerosis. *The Lancet*. 2008;372(9639):657–68.
- Curatolo P, Moavero R, de Vries PJ. Neurological and neuropsychiatric aspects of tuberous sclerosis complex. *Lancet Neurol*. 2015;14(7):733–45.
- Northrup H, Aronow ME, Bebin EM, Bissler J, Darling TN, de Vries PJ, Frost MD, Fuchs Z, Gosnell ES, Gupta N, et al. Updated international tuberous sclerosis complex diagnostic criteria and surveillance and management recommendations. *Pediatr Neurol*. 2021;123:50–66.
- Liu S, Yu T, Guan Y, Zhang K, Ding P, Chen L, Shan Y, Guo Q, Liu Q, Yao Y, et al. Resective epilepsy surgery in tuberous sclerosis complex: a nationwide multicentre retrospective study from China. *Brain*. 2020;143(2):570–81.
- West S, Nevitt SJ, Cotton J, Gandhi S, Weston J, Sudan A, Ramirez R, Newton R. Surgery for epilepsy. *Cochrane Database Syst Rev*. 2019;6:CD010541.
- Ma TS, Elliott RE, Ruppe V, Devinsky O, Kuzniecky R, Weiner HL, Carlson C. Electrographic evidence of perituberal cortex epileptogenicity in tuberous sclerosis complex. *J Neurosurg Pediatr*. 2012;10(5):376–82.
- Krsek P, Jahodova A, Kyncl M, Kudr M, Komarek V, Jezdik P, Jayakar P, Miller I, Korman B, Rey G, et al. Predictors of seizure-free outcome after epilepsy surgery for pediatric tuberous sclerosis complex. *Epilepsia*. 2013;54(11):1913–21.
- Shao X, Zhang X, Xu W, Zhang Z, Zhang J, Guo H, Jiang T, Zhang W. Neurite orientation dispersion and density imaging parameters may help for the evaluation of epileptogenic tubers in tuberous sclerosis complex patients. *Eur Radiol*. 2021;31(8):5605–14.
- Wang Y, Yuan L, Zhang S, Liang S, Yu X, Liu T, Yang X, Liang S. Fast ripples as a biomarker of epileptogenic tuber in tuberous sclerosis complex patients using stereo-electroencephalograph. *Front Hum Neurosci*. 2021;15:680295.
- Shan W, Mao X, Wang X, Hogan RE, Wang Q. Potential surgical therapies for drug-resistant focal epilepsy. *CNS Neurosci Ther*. 2021;27:994–1011.
- Steinbrenner M, Duncan JS, Dickson J, Rathore C, Wächter B, Aygun N, Menon RN, Radhakrishnan A, Holtkamp M, Ilyas-Feldmann M. Utility of ¹⁸F-fluorodeoxyglucose positron emission tomography in presurgical evaluation of patients with epilepsy: a multicenter study. *Epilepsia*. 2022;63(5):1238–52.
- Zhou H, Zhang W, Tan Z, Zhou Z, Li Y, Zhang S, Zhang L, Gan J, Wu H, Tang Y, et al. Localizing epileptic foci before surgery in patients with MRI-Negative refractory epilepsy using statistical parameter mapping and three-dimensional stereotactic surface projection based on (18)F-FDG PET. *Front Bioeng Biotechnol*. 2021;9:810890.
- Beheshti I, Sone D, Maikusa N, Kimura Y, Shigemoto Y, Sato N, Matsuda H. Accurate lateralization and classification of MRI-negative 18F-FDG-PET-positive temporal lobe epilepsy using double inversion recovery and machine-learning. *Comput Biol Med*. 2021;137:104805.
- Zhao Z, Li H, Wang S, Chen C, He C, Hu L, Zheng Z, Zhu J, Ding M, Wang S, et al. Patterns of hypometabolism in frontal lobe epilepsy originating in different frontal regions. *Ann Clin Transl Neurol*. 2022;9(9):1336–44.
- Ding Y, Zhu Y, Jiang B, Zhou Y, Jin B, Hou H, Wu S, Zhu J, Wang Z, Wong CH, et al. (18)F-FDG PET and high-resolution MRI co-registration for pre-surgical evaluation of patients with conventional MRI-negative

- refractory extra-temporal lobe epilepsy. *Eur J Nucl Med Mol Imaging*. 2018;45(9):1567–72.
16. Subramaniam T, Jain A, Hall LT, Cole AJ, Westover MB, Rosenthal ES, Struck AF. Lateralized periodic discharges frequency correlates with glucose metabolism. *Neurology*. 2019;92(7):e670–4.
 17. Wang Z, Huang K, Yang X, Shen K, Yang L, Ruan R, Shi X, Wang M, Zhu G, Yang M, et al. Downregulated GPR30 expression in the epileptogenic foci of female patients with focal cortical dysplasia type IIb and tuberous sclerosis complex is correlated with (18) F-FDG PET-CT values. *Brain Pathol*. 2021;31(2):346–64.
 18. Chari A, Sedlacik J, Seunarine K, Piper RJ, Hales P, Shmueli K, Mankad K, Löbel U, Eltze C, Moeller F, et al. Epileptogenic Tubers Are Associated with Increased Kurtosis of Susceptibility Values: a combined quantitative susceptibility mapping and Stereoelectroencephalography Pilot Study. *Am J Neuroradiol*. 2023;44(8):974–82.
 19. Liang S, Zhang J, Yang Z, Zhang S, Cui Z, Cui J, Zhang J, Liu N, Ding P. Long-term outcomes of epilepsy surgery in tuberous sclerosis complex. *J Neurol*. 2017;264(6):1146–54.
 20. Zhang M-N, Zou L-P, Wang Y-Y, Pang L-Y, Ma S-F, Huang L-L, Gao Y, Lu Q, Franz DN. Calcification in cerebral parenchyma affects pharmacoresistant epilepsy in tuberous sclerosis. *Seizure*. 2018;60:86–90.
 21. Orhac F, Soussan M, Maisonnobe J-A, Garcia CA, Vanderlinden B, Buvat I. Tumor Texture Analysis in 18F-FDG PET: relationships between texture parameters, histogram indices, standardized uptake values, metabolic volumes, and total lesion glycolysis. *J Nucl Med*. 2014;55(3):414–22.
 22. Abd El-Hafez YG, Moustafa HM, Khalil HF, Liao C-T, Yen T-C. Total lesion glycolysis: a possible new prognostic parameter in oral cavity squamous cell carcinoma. *Oral Oncol*. 2013;49(3):261–8.
 23. Mertens J, Dobbeleir A, Ham H, D'Asseler Y, Goethals I, Van de Wiele C. Standardized added metabolic activity (SAM): a partial volume independent marker of total lesion glycolysis in liver metastases. *Eur J Nucl Med Mol Imaging*. 2012;39(9):1441–8.
 24. Yokota H, Uetani H, Tatekawa H, Hagiwara A, Morimoto E, Linetsky M, Yoo B, Ellingson BM, Salamon N. Focal cortical dysplasia imaging discrepancies between MRI and FDG-PET: Unique association with temporal lobe location. *Seizure*. 2020;81:180–5.
 25. Yasin SA, Ali AM, Tata M, Picker SR, Anderson GW, Latimer-Bowman E, Nicholson SL, Harkness W, Cross JH, Paine SM, et al. mTOR-dependent abnormalities in autophagy characterize human malformations of cortical development: evidence from focal cortical dysplasia and tuberous sclerosis. *Acta Neuropathol*. 2013;126(2):207–18.
 26. Quigg M, Kundu B. Dynamic FDG-PET demonstration of functional brain abnormalities. *Ann Clin Transl Neurol*. 2022;9(9):1487–97.
 27. Zhang M, Qin Q, Zhang S, Liu W, Meng H, Xu M, Huang X, Lin X, Lin M, Herman P, et al. Aerobic glycolysis imaging of epileptic foci during the inter-ictal period. *eBioMedicine*. 2022;79:104004.
 28. Aslam S, Damodaran N, Rajeshkannan R, Sarma M, Gopinath S, Pillai A. Asymmetry index in anatomically symmetrized FDG-PET for improved epileptogenic focus detection in pharmacoresistant epilepsy. *J Neurosurg*. 2023;138(3):828–36.
 29. Liu S, Cai Y, Rong R, Hu P, Chen S, Wang X, Shi H. Tuberous sclerosis complex (TSC) with epilepsy on (18)F-FDG simultaneous PET/MR. *Eur J Nucl Med Mol Imaging*. 2020;47(10):2471–2.
 30. Asano E, Chugani DC, Muzik O, Behen M, Janisse J, Rothermel R, Mangner TJ, Chakraborty PK, Chugani HT. Autism in tuberous sclerosis complex is related to both cortical and subcortical dysfunction. *Neurology*. 2001;57(7):1269–77.
 31. Wu JY, Salamon N, Kirsch HE, Mantle MM, Nagarajan SS, Kurelowech L, Aung MH, Sankar R, Shields WD, Mathern GW. Noninvasive testing, early surgery, and seizure freedom in tuberous sclerosis complex. *Neurology*. 2010;74(5):392–8.
 32. Chandra PS, Salamon N, Huang J, Wu JY, Koh S, Vinters HV, Mathern GW. FDG-PET/MRI coregistration and diffusion-tensor imaging distinguish epileptogenic tubers and cortex in patients with tuberous sclerosis complex: a preliminary report. *Epilepsia*. 2006;47(9):1543–9.
 33. Tang Y, Yu J, Zhou M, Li J, Long T, Li Y, Feng L, Chen D, Yang Z, Huang Y, et al. Cortical abnormalities of synaptic vesicle protein 2A in focal cortical dysplasia type II identified in vivo with (18)F-SynVesT-1 positron emission tomography imaging. *Eur J Nucl Med Mol Imaging*. 2022;49(10):3482–91.
 34. Sinclair B, Cahill V, Seah J, Kitchen A, Vivash LE, Chen Z, Malpas CB, O'Shea MF, Desmond PM, Hicks RJ, et al. Machine learning approaches for imaging-based prognostication of the outcome of surgery for mesial temporal lobe epilepsy. *Epilepsia*. 2022;63(5):1081–92.
 35. Cilla S, Macchia G, Lenkowicz J, Tran EH, Pierro A, Petrella L, Fanelli M, Sardu C, Re A, Boldrini L, et al. CT angiography-based radiomics as a tool for carotid plaque characterization: a pilot study. *Radiol Med*. 2022;127(7):743–53.
 36. Lin J, Ding S, Li X, Hua Y, Wang X, He R, Du Y, Xia N, Chen Y, Zhu Z, et al. External validation and comparison of two prediction models for seizure recurrence after the withdrawal of antiepileptic drugs in adult patients. *Epilepsia*. 2020;61(1):115–24.
 37. Yang S, Han X, Wang N, Gu R, Chen W, Wang E, Chen Y, He G, Zhu X, Ma B, et al. Predicting seizure freedom with AED treatment in newly diagnosed patients with MRI-negative epilepsy: A large cohort and multicenter study. *Epilepsy Behav*. 2020;106:107022.
 38. Rubi S, Costes N, Heckemann RA, Bouvard S, Hammers A, Marti Fuster B, Ostrowsky K, Montavont A, Jung J, Setoain X, et al. Positron emission tomography with alpha-[11C]methyl-L-tryptophan in tuberous sclerosis complex-related epilepsy. *Epilepsia*. 2013;54(12):2143–50.
 39. Kagawa K, Chugani DC, Asano E, Juhasz C, Muzik O, Shah A, Shah J, Sood S, Kupsky WJ, Mangner TJ, et al. Epilepsy surgery outcome in children with tuberous sclerosis complex evaluated with alpha-[11C]methyl-L-tryptophan positron emission tomography (PET). *J Child Neurol*. 2005;20(5):429–38.
 40. Chugani DC. α -methyl-L-tryptophan: mechanisms for tracer localization of epileptogenic brain regions. *Biomark Med*. 2011;5(5):567–75.
 41. Kumar A, Asano E, Chugani HT. α -[11C]-methyl-L-tryptophan PET for tracer localization of epileptogenic brain regions: clinical studies. *Biomark Med*. 2011;5(5):577–84.

Publisher's Note

Springer Nature remains neutral with regard to jurisdictional claims in published maps and institutional affiliations.

Ready to submit your research? Choose BMC and benefit from:

- fast, convenient online submission
- thorough peer review by experienced researchers in your field
- rapid publication on acceptance
- support for research data, including large and complex data types
- gold Open Access which fosters wider collaboration and increased citations
- maximum visibility for your research: over 100M website views per year

At BMC, research is always in progress.

Learn more biomedcentral.com/submissions

